

Rippling Instability of a Collapsing Bubble

Rava da Silveira*, Sahraoui Chaieb† and L. Mahadevan†

**Department of Physics*, †*Department of Mechanical Engineering*

Massachusetts Institute of Technology, 77 Mass Ave., Cambridge, MA 02139, U.S.A.

Abstract

When a bubble of air rises to the top of a highly viscous liquid, it forms a dome-shaped protuberance on the free surface. Unlike a soap bubble, it bursts so slowly as to collapse under its own weight simultaneously, and folds into a striking wavy structure. This rippling effect occurs in fact for both elastic and viscous sheets, and a theory for its onset is formulated. The growth of the corrugation is governed by the competition between gravitational and bending (shearing) forces and is exhibited for a range of densities, stiffnesses (viscosities), and sizes – a result which arises less from dynamics than from geometry, suggesting a wide validity. A quantitative expression for the number of ripples is presented, together with experimental results which are in agreement with the theoretical predictions.

Every day, nature surprises us with structures and patterns of such beauty as to fill the scientist with wonder and the artist with envy. In the present paper, we address an instability which turns a hemispherical, smooth, liquid bubble into a striking wrinkled structure, first observed by Debrégeas, de Gennes, and Brochard-Wyart [1]. In their experiment, 0.1 to 10 cm^3 of air injected into a highly viscous liquid ($\eta \sim 10^3 \text{ Pa}\cdot\text{s}$) rises to the free surface, imprisoned in a hemispherical bubble of thickness $t \sim 1 - 10 \mu\text{m}$. If the latter is punctured at its apex by a needle, surface tension drives the rapid expansion of a circular opening. The retraction velocity soon (after about $10 - 30 \text{ ms}$) saturates to a constant, owing to the high viscous resistance. In the meantime, the air flow through the hole equilibrates the pressure difference, allowing the bubble to collapse under its own weight. As it deflates, an *instability* appears: the fluid sheet folds into a wavy structure, with radial ripples that break the original axisymmetry. In the absence of a detailed theory, Ref. [1] proposes a scaling estimate for the number of ripples $n^* \sim (\mu g R^3 / K)^{1/2}$, where μ is the mass of the film per unit area, g the gravitational acceleration, R the radius of the hole, and K an effective bending rigidity of the sheet which was assumed to be elastic during the early stages of the rippling.

The rippling results from the competition between compression, bending, and gravity. Each fluid element tends to fall under its own weight, but experiences a viscous resistance from its neighborhood. If the bubble were to collapse in a uniform, symmetric way, it would occupy a progressively reduced area, leading to an in-plane compression which would require forces that far exceed the scale set by gravity. Instead, the film deforms in a nearly inextensional fashion by undergoing pure bending. Equivalently, for a given (gravitational) force, the relative time scale associated with stretching is much larger than that for bending, and the surface therefore corrugates over short times, before eventually relaxing into a uniform, thicker membrane.

This instability is reminiscent of buckling phenomena [2], originally studied in the context of elastic rods but occurring also in the creeping flows of viscous liquid filaments (a

striking everyday example being the coiling of a stream of honey when it reaches a toast [3,4]). For an elastic rod, buckling occurs at the longest possible wavelength in order to minimize the bending energy. In the bubble problem, however, gravity plays a distinctive role in determining the configuration. For a given amplitude, bending still favors large scale deformations, while gravitational energy is minimized for an almost flat sheet with as many tiny ripples as possible; the optimal wavelength results from a compromise between the two. Such an argument, however, does not fully characterize the effect. Unlike the above examples, here the system under consideration is a *curved two-dimensional* sheet, and the associated geometry constrains the rippling both qualitatively and quantitatively, as we shall see.

The instability occurs both an elastic (solid) film and a viscous (liquid) one. The elastic case corresponds to a convex curved shell with an apical hole of radius R that is allowed to collapse under its own weight. In the viscous case, an additional complication arises because the radius of the hole changes during the rippling. Following a short initial transient, the hole grows steadily at a rate $v \sim \sigma/\eta$ resulting from the balance of surface tension ($\sigma \approx 20 \text{ mN/m}$) and viscous stress. It thus takes a time $\tau \sim \eta t/\sigma$ for the opening radius to increase by t . During this time, the liquid acquires a velocity $V \sim g\tau$ due to gravity, larger than v by a factor $V/v \sim 10^7$. Even if the liquid is viscoelastic, so that the retraction velocity is enhanced by a factor R/t ($\sim 10 - 10^4$) [5,1], the hole radius remains essentially constant while the instability occurs (*cf.* Fig. 1). We may therefore treat the hole radius R as a given parameter in the theory [6].

Although the bubble has the geometry of a sphere before collapsing, it is quite flattened by the time the ripples appear (Fig. 1(B)). For simplicity, we consider the unperturbed configuration to be a shallow cone, of slope $\alpha \ll 1$, described by its height above the surface,

$$h = \alpha(r_0 - r), \quad (1)$$

where r is the cylindrical radial coordinate and r_0 the radius of the base. Any deformation

of h introduced by the rippling may be written, without loss of generality, as

$$h + \delta h = \alpha(r_0 - r) - \delta\alpha(r) + \sum_{n \geq 1} \left\{ \delta\beta_n^{(1)}(r) \cos(n\theta) + \delta\beta_n^{(2)}(r) \sin(n\theta) \right\}, \quad (2)$$

where θ is the azimuthal angle. The perturbation $\delta\alpha$ represents a uniform (n independent) flattening accompanying the growth of ripples of amplitude $\delta\beta_n^{(i)}$, and a crucial step consists in understanding their form and interdependence. In the case of a thin elastic (viscous) sheet, the two primary modes of deformation are in-plane stretching (shearing) and out-of-plane bending. A generic deformation of an elastic cone (made of a material with Young modulus Y), of amplitude ζ on a scale ℓ , requires stretching forces (per unit surface) of order $Yt\zeta^2/\ell^2$, but significantly smaller stretching forces (per unit surface) of order $Yt^3\zeta^2/\ell^4$ [7], so that for a given external force, here gravity, inextensional deformations are greatly preferred [8]. In the case of a highly viscous sheet, forces arise from velocity gradients, thus introducing a dynamical element in the problem. However, their dependence on t and ℓ (essentially due to the variation of the strain across the film) is similar, so that inextensional deformations are again largely favored if $t \ll l \approx r_0/n^*$. (This condition is satisfied if the selected number of ripples n^* is small compared to 10^3 , which is the case as we shall see below.) Equivalently, for a given loading, the time scale corresponding to bending is smaller than that for stretching by a factor $(t/l)^2$ [9,10]. Thus, at the onset of the instability, perturbations of the cone must preserve its metric. This requirement translates into the constraints [11]

$$\delta\beta_n^{(i)}(r) = \delta\beta_n^{(i)} \times r + \delta\beta_n^{(i)\prime}, \quad (3)$$

(where $\delta\beta_n^{(i)}$ and $\delta\beta_n^{(i)\prime}$ are constants) and

$$4\alpha\delta\alpha(r) = \sum_{n \geq 1, i} \left\{ (n^2 - 1) \delta\beta_n^{(i)2} (r - r_0) + n^2 \delta\beta_n^{(i)\prime 2} \left(\frac{1}{r} - \frac{1}{r_0} \right) \right\}. \quad (4)$$

In the following, we elucidate the elastic (solid) case before extending our treatment to the viscous (liquid) case. The energy functional of a perturbed elastic cone reads

$$\begin{aligned} E[h + \delta h] &= \int_{\text{cone}} d(\text{surface}) \times (\text{gravitational potential energy} + \text{bending potential energy}) \\ &= \int_R^{r_0} r dr \int_0^{2\pi} d\theta \sqrt{1 + [\nabla(h + \delta h)]^2} \left\{ \mu g(h + \delta h) + \frac{K}{2} (\nabla^2 \delta h)^2 \right\}. \end{aligned} \quad (5)$$

where $K = Yt^3/12(1 - \nu^2)$ is the rigidity and ν the Poisson ratio. Only bending elastic energy appears in E , since we have confined ourselves to the class of inextensible deformations.

If the elastic cone is attached to the plane on which it rests so that $\delta h(r = r_0) = 0$, Eq. (3) yields $\delta\beta_n^{(i)\prime} = -\delta\beta_n^{(i)}r_0$. On substituting Eqs. (2–4) into Eq. (5) we then obtain, to lowest order in the perturbation,

$$\begin{aligned}\delta E &\equiv E[h + \delta h] - E[h] \\ &= \frac{\pi}{2}K \cdot f\left(\frac{r_0}{R}\right) \cdot \sum_{n \geq 1, i} \left(\delta\beta_n^{(i)}\right)^2 \left\{ g\left(\frac{r_0}{R}, \gamma R^3\right) + 2 \left[\varphi\left(\frac{r_0}{R}\right) - \gamma R^3 \psi\left(\frac{r_0}{R}\right) \right] n^2 + n^4 \right\} \\ &\equiv \sum_{n \geq 1} \delta E_n.\end{aligned}\tag{6}$$

$\gamma^{-1/3} = (\alpha K/\mu g)^{1/3}$ is an intrinsic length scale arising from the competition between gravity and bending elasticity [12].

Each mode contributes an amount δE_n to the change in energy, and rippling occurs if $\delta E_n < 0$ for some integer. In general, $\delta E_n < 0$ for a range of different n 's; the most negative variation corresponds to the maximally growing perturbation, and thus sets the wavelength of the instability. The formulation also yields a “threshold condition” $\varphi(r_0/R) < \gamma R^3 \psi(r_0/R)$ for the occurrence of rippling. This condition involves the three independent quantities γ , r_0 , and R , and may be translated into three corresponding statements. (i) Rippling is suppressed if $\gamma < \gamma_c(r_0, R) = R^{-3}\varphi/\psi$, *i.e.* if the cone is too light or too rigid. (ii) Similarly, no rippling occurs if the hole, or equivalently the cone, is too small, $r_0 < r_{0c}(\gamma, R)$. Azimuthal continuity requires the wavelength of the deformation to be at most of order r_0 , resulting in a forbidding bending cost if r_0 becomes small compared to the intrinsic (energetically determined) scale $\gamma^{-1/3}$. (iii) Finally, the threshold depends, quite unexpectedly, on the *ratio* r_0/R . The dependence of the symmetric ($n = 0$) mode on the radial coordinate r is different from that of the rippling ($n \neq 0$) modes, so that the high elastic cost cannot be justified by gravitational gain anymore if the hole is reduced beyond a critical size. Minimizing δE in Eq. (6) yields the selected number of ripples as

$$n^* = \text{Int} \sqrt{\frac{\mu g R^3}{K} \cdot \frac{1}{\alpha} \psi \left(\frac{r_0}{R} \right) - \varphi \left(\frac{r_0}{R} \right)}, \quad (7)$$

where $\text{Int}\{x\}$ is the integer closest to x . This relation improves on the estimate of Ref. [1], where the authors consider the short time elastic behavior, and establishes its domain of validity.

For an elastic (solid) sheet, the rippling phenomenon is of an essentially static nature; upon increasing, say, the mass of the sheet, the equilibrium configuration is shifted from symmetric to rippled. Approaching the problem from a dynamical perspective by considering the elastic forces and torques rather than the corresponding energies results in an evolution equation $\pi \mu P(r_0, R) \cdot d^2(\delta \beta_n^{(i)})/dt^2 = -\delta E/\delta \beta_n^{(i)}$ for each mode. Here P is a polynomial function independent of n , so that the energetically optimal mode, with number n^* , is indeed the fastest growing one. In the case of a viscous liquid, the effect is intrinsically dynamical: bending occurs only on short times, while the equilibrium configuration is ultimately reached by a slow thickening. Nevertheless, the motion of a viscous film satisfies a formulation close to that of an elastic sheet, as can be shown by integrating the Stokes equation through the thickness [10,13]. Indeed, it is easy to see that bending results from a torque $\frac{\eta t^3}{4(1-\nu^2)} \times d(\text{curvature})/dt$ analogous to an elastic torque $K \times (\text{curvature})$, so that a highly viscous film may be described by an effective bending modulus $K_l = \eta t^3/3\tau$ ($\nu = 1/2$ for an incompressible medium), where τ is a time scale associated with the falling velocity. Thus, all the conclusions of the stability analysis for the elastic cone, and in particular the expression for the number of ripples (Eq. (7)), may be transposed to the case of the bubble modulo a certain time scale related to the gravity-induced velocity of the fluid. Comparing the nascent ripples' amplitude to the film thickness yields an estimate of this time scale as $(t/g)^{1/2}$ [14].

In order to check our results against experiment, we visualized the bursting of silicone oil bubbles. Once the bubble is punctured with a sharp needle, its evolution is followed using a high-speed camera capable of recording up to 1000 frames per second. The resulting video is then analyzed to determine the radius r_0 of the bubble, the hole size R at which the ripples are first observed, along with the number of ripples n^* . Since the hole expands

very fast at first, R is much larger than R_c by the time the bubble begins to collapse. To compare the experiments with the theory, in which R enters as a parameter, the latter is measured at the onset of the instability for each given size of the bubble. The quantitative measurements are compared to the theoretical predictions for the dependence of n^* on the bubble size on Fig. 2. On a more qualitative level, the experiments show a suppression of the instability for small bubbles, in agreement with the threshold conditions above.

We conclude with a discussion of possible refinements of the theory and their relation to the geometric nature of the problem. A more complete theory would incorporate a (flattened) hemisphere as the initial condition, rather than a cone. Also, due to the progressive drainage of the liquid, the thickness t acquires a dependence on r (and time). This in turn implies non-uniform rigidity $K(r)$ and mass $\mu(r)$, leading to functions f , g , φ , ψ , and P of a more complicated form. On a more fundamental level, all these aspects should be addressed in terms of the coupled hydrodynamics of the slow viscous (liquid) flow and the rapid air flow; the corresponding calculations will be reported elsewhere [13]. Yet, the strong geometrical constraints involved in the problem are suggestive of the robustness of the results. The question we have answered is akin to that of applying a curved surface unto a flat one in the most economical way, a problem which has taxed cartographers for many centuries and lies at the birth of differential geometry. It is also somewhat of an inverse counterpart to the problem of fitting a flat sheet to a three dimensional landscape, which has been studied in various contexts [15–17], and is an issue that still vexes fashion designers. The relevance of the geometrical constraints is manifest, for example, in the strong dependence of the rippling on the size of the opening, which is closely related to a well-known theorem due to Gauss [18], Jellett [19], and others, according to which (loosely put) a closed surface cannot be bent without being stretched, while an open surface can be bent inextensionally. Similarly, we find that a smaller hole implies a relatively stiffer bubble, and hampers the rippling. While the detailed form of the functions φ and ψ arise from the physical constraints and dynamics imposed by the forces and various boundary conditions, the essence is in the geometry.

REFERENCES

- [1] G. Debrégeas, P.-G. de Gennes, and F. Brochard-Wyart, *Science* **279**, 1704 (1998).
- [2] D. Brush and B. Almroth, *Buckling of bars, plates and shells* (McGraw-Hill, New York, 1975).
- [3] G. I. Taylor, *Proc. 12th Intl Congr. Appl. Mech.*, 382 (1969).
- [4] L. Mahadevan, W. S. Ryu, and A. D. T. Samuel, *Nature* **392**, 140 (1998).
- [5] G. Debrégeas, P. Martin, and F. Brochard-Wyart, *Phys. Rev. Lett.* **75**, 3886 (1995).
- [6] While surface tension drives the expansion of the hole, rippling is dominated by gravity and viscosity, and we neglect any surface tension-related considerations in the remainder.
- [7] For a review of elasticity theory, see L. D. Landau and E. M. Lifshitz, *Theory of Elasticity*, 3rd Edn. (Pergamon, New York, 1986) and A. E. H. Love, *A Treatise on the Mathematical Theory of Elasticity*, 4th Edn. (Dover, New York, 1944).
- [8] The fact that the unperturbed surface is curved plays an essential role here. For a plane, bending energy dominates in the limit a small deformation, with respect to stretching. (For more details, see Ref. [7].)
- [9] J. D. Buckmaster, A. Nachman, and L. Ting, *J. Fluid Mech.* **69**, 1 (1975).
- [10] P. D. Howell, *Eur. J. of App. Math.* **7**, 321 (1996).
- [11] Exact inextensibility requires that each point on the surface be displaced in the three dimensions in which the cone is imbedded: vertical, radial, and azimuthal. Of course, the three displacements are coupled, and, in the limit $\alpha \ll 1$, the radial and angular components are negligibly smaller (by a factor α) than the vertical deformation. Also, we note that the form of these “inextensibility conditions” depends on the unperturbed configuration, which, in particular, is curved.

[12] Here

$$\varphi(x) = \frac{2(x-1-\ln x)}{x^2-4x+3+2\ln x} \geq 0, \quad \psi(x) = \frac{(x-1)^3}{3(x^2-4x+3+2\ln x)} \geq 0 \quad (\text{for } x \in [1, \infty]),$$

and $f(x)$, $g(x, y)$ are similar rational functions of x , $\ln x$, and y .

[13] R. da Silveira, S. Chaïeb, and L. Mahadevan, in preparation.

[14] As the bubble continues to fall, this time scale may vary and so may the number of ripples. However, this last possibility is unlikely owing to the large forces required to introduce new ripples or remove existing ones.

[15] Y. Kantor, M. Kardar, and D. R. Nelson, Phys. Rev. Lett. **57**, 791 (1986).

[16] A. Lobkovksy, S. Gentges, H. Li, D. Morse and T. Witten, Science **270**, 1482 (1995).

[17] E. Cerda, S. Chaïeb, F. Melo, and L. Mahadevan, Nature **401**, 46 (1999).

[18] M. Spivak, *A Comprehensive Introduction to Differential Geometry*, vol. I, 2nd Edn. (Publish or Perish, 1979).

[19] J. H. Jellett, Dublin Roy. Irish Acad. Trans. **22** (1855).

[20] R.d.S. wishes to thank Georges Debrégeas for introducing him to the problem and sharing enthusiasm and insight. He is also very grateful to Professor Mehran Kardar for his precious guidance and comments. S.C. thanks Professor Gareth McKinley for his support. This work was supported by the NSF grant No. DMR-98-05833 (R.d.S.), the NASA grant No. NAG3-2155 (S.C.), and the Karl van Tassel Chair at MIT (L.M.).

FIG. 1. Stroboscopic images of a collapsing liquid bubble of size is $r_0 = 1\text{cm}$ and thickness $t \approx 100\mu\text{m}$. The silicone oil has viscosity $\eta = 10^3\text{Pa}\cdot\text{s}$, surface tension $\sigma = 21\text{mN/m}$, and mass density 0.98g/cm^3 . (A) 30ms after the film is punctured by a sharp needle, the bubble shows a retracting hole of radius $R = 1.4\text{mm}$ at its apex, but no ripples yet. (B) 30ms later, the bubble loses its axisymmetric shape. The radius of the hole remains essentially constant, at $R = 1.6\text{mm}$, while the ripples grow. The inset displays a schematic side view of the essentially conical deflating bubble at the onset of the instability, with the important quantities involved in the phenomenon. The extreme shallowness allows for a perturbative treatment in the slope α of the cone.

FIG. 2. Plot of the number of ripples n^* as a function of the bubble radius r_0 , comparing the experimental measures (points) with the theoretical predictions (solid lines). These data were gathered using silicone oil of viscosity $\eta = 600\text{Pa}\cdot\text{s}$ and bubbles of thickness $t \approx 30\mu\text{m}$. The errors in the measurement of r_0 arise from meniscus effects which are more important in smaller bubbles. The bursting time elapsed up to rippling is measured to be of order of 1 to 5 times $(t/g)^{1/2}$, consistent with our proposed mechanism for the formation of the corrugation. For each experimental realization, the ratio r_0/R was measured at the onset of the instability, and the corresponding dependence of R on r_0 was used to get a theoretical curve $n^* = n^*(r_0)$. The thinner line displays the prediction for an elastic sheet attached to the plane on which it rests. The liquid, however, can in no way be clamped, and one has to relax the boundary conditions at the base. This leads to a vanishing of the unprimed modes (*cf.* Eq. (3)), which are unfavorable in terms of both gravitational and viscous forces; the fastest growing primed modes lead to the behavior represented by the thicker line. The latter is plotted here for a slope $\alpha \approx 3^\circ (\approx 0.05\text{rad})$ of the cone, consistent with our perturbative treatment, and in agreement with direct observation. The dashed line represents the best fit of the scaling form $n^* \sim (\mu g R^3/K)^{1/2}$ [1], where R is chosen as the relevant length scale. If R is replaced by r_0 , the above expression for n^* may be closely fitted (up to an

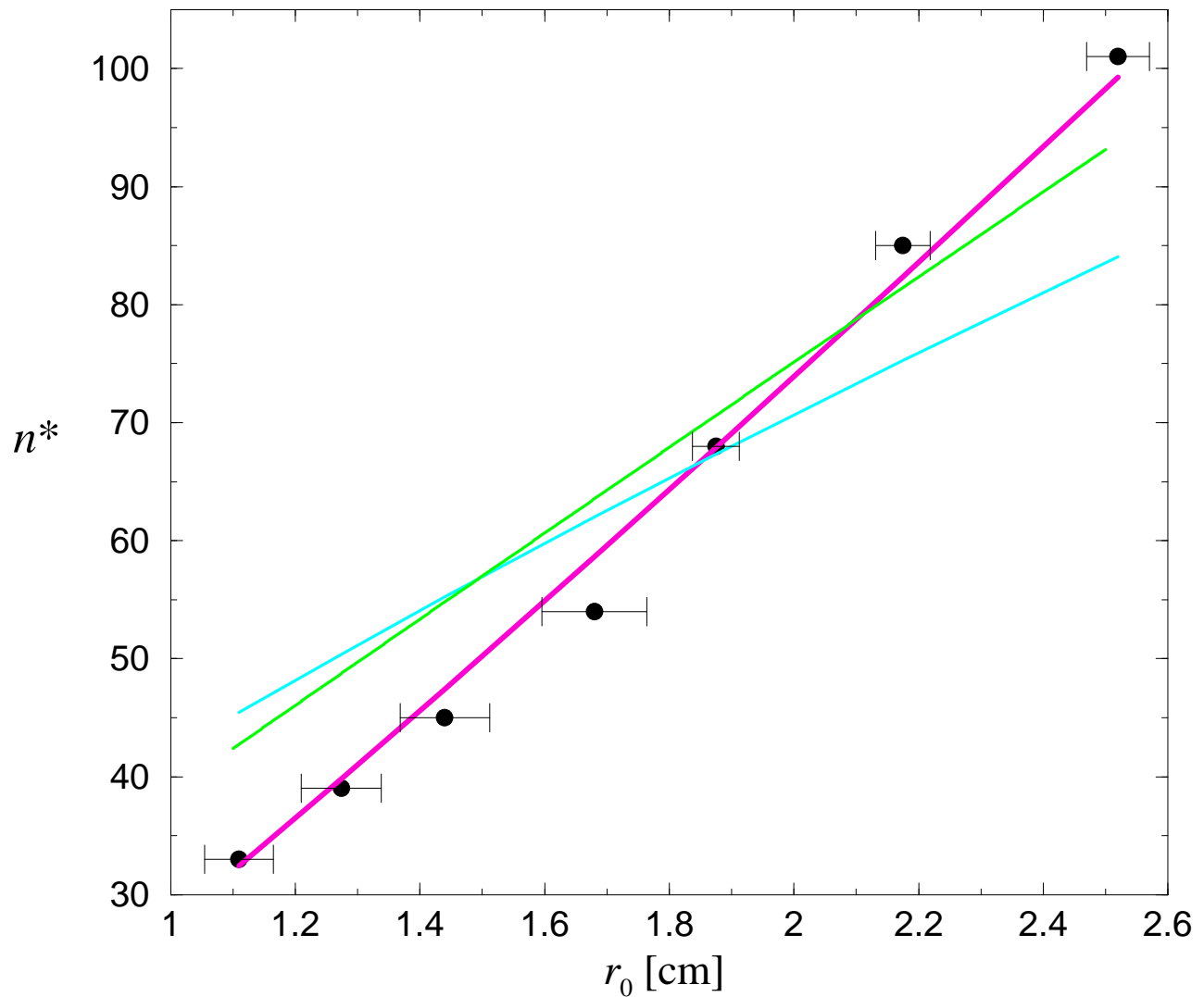
overall multiplicative factor) to our predicted curve, showing that the size of the bubble is the dominant length scale within the present experimental range and conditions. This is consistent with the relaxed boundary conditions, which allow the ripples to be significant close to the outer edge of the bubble (*cf.* also Fig. 1.(B)). In this way, the ripples trade a bulk gain in gravitational and bending stresses against a cost in stretching in a thin rim close to the outer edge. The increased thickness of the liquid film close to the base further emphasizes this effect, as it reduces the difference in magnitude between a typical stretching and a typical bending stress. The inset shows a top view of the fully developed ripples, from which n^* is measured.

This figure "bubble_after.jpg" is available in "jpg" format from:

<http://arxiv.org/ps/cond-mat/0008175v1>

This figure "bubble_before.jpg" is available in "jpg" format from:

<http://arxiv.org/ps/cond-mat/0008175v1>



This figure "bubble_top.jpg" is available in "jpg" format from:

<http://arxiv.org/ps/cond-mat/0008175v1>